Simen Owen Academic Proceedings Series

Vol. 3 2026

Article **Open Access**

Energy-Adaptive Micro-Mechanical Systems Driven by Intelligent Materials: Experimental and Simulation Study Based on the Piezoelectric Effect

Zhengjie Chen [1,*]

[1] Shanghai Boda School Paddington Center for International Curriculum, Shanghai, 201620, China
* Correspondence: Zhengjie Chen, Shanghai Boda School Paddington Center for International Curriculum, Shanghai, 201620, China

Abstract: The miniaturization of mechanical and electronic systems has driven demand for self-powered micro-electro-mechanical systems (MEMS) in robotics, biomedical implants, and distributed IoT networks. Piezoelectric materials offer direct mechanical-to-electrical energy conversion, making them promising candidates for energy-autonomous microsystems. Existing studies largely optimize either material performance or system-level design independently, neglecting the integration of microstructural electromechanical behavior with adaptive energy regulation. Moreover, nonlinear piezoelectric responses under micro-scale cyclic loading remain insufficiently quantified, leading to 15-30% discrepancies between simulations and experiments. This work develops a hybrid PZT-PVDF composite thin film integrated into a cantilever MEMS with a closed-loop adaptive feedback controller. A coupled multi-physics finite element model links stress-strain fields to voltage output, while real-time stiffness adjustment maximizes energy harvesting efficiency under variable vibration conditions. Experimental validation spans 150 samples with cyclic loading across 50-500 Hz. The proposed adaptive MEMS achieves a peak voltage of 5.8 ± 0.2 V, output power density of 2.45 ± 0.05 mW·cm^{-3}, and conversion efficiency of 77.1 ± 1.1%, representing a 28% improvement over non-adaptive hybrid systems. Voltage degradation after 10^5 cycles is limited to 3.2 ± 0.4%, and the system converges to steady-state power within 12 ± 2 control iterations. By integrating material-level physics, multi-physics modeling, and adaptive control, this framework enhances energy conversion reliability and provides a reproducible approach for designing energy-autonomous MEMS suitable for micro-robots, implantable sensors, and distributed IoT devices.

Keywords: energy-adaptive MEMS; piezoelectric composites; multi-physics modeling; adaptive feedback control

Received: 24 December 2025
Revised: 02 February 2026
Accepted: 15 February 2026
Published: 18 February 2026

1. Introduction

The rapid miniaturization of mechanical and electronic components has accelerated the development of micro-electro-mechanical systems (MEMS) capable of sensing, actuation, and energy conversion at sub-millimeter scales [1]. As the demand for autonomous microsystems in robotics, biomedical implants, and distributed Internet-of-Things (IoT) networks increases, the need for sustainable, self-powered mechanisms becomes increasingly critical [2]. Conventional MEMS often rely on external power sources or limited-capacity microbatteries, which restrict long-term operation and scalability [3]. Intelligent materials, particularly those exhibiting piezoelectric, triboelectric, or electrostrictive properties, offer a promising route for enabling self-

adaptive energy management. Among them, piezoelectric materials stand out due to their direct mechanical-to-electrical energy conversion capability, high responsiveness, and compatibility with microfabrication processes [4].

Despite significant advances in piezoelectric MEMS, several limitations remain. Most existing studies focus on improving either material-level performance (e.g., polarization, alignment, or fatigue resistance) or system-level control (e.g., resonance tuning, load matching) in isolation, with limited integration between the two [5]. Furthermore, while piezoelectric coupling mechanisms are well understood in macro-scale actuators, their nonlinear behavior under micro-scale cyclic stress and variable boundary conditions is insufficiently quantified. Current models frequently simplify electro-mechanical interactions by assuming constant coupling coefficients or neglecting thermal and geometric nonlinearities [6]. Consequently, discrepancies persist between simulated and experimental performance, particularly in energy conversion efficiency and dynamic stability. These challenges hinder the practical deployment of piezoelectric MEMS in adaptive energy harvesting and real-time control applications.

To address these issues, this study aims to establish a unified framework linking material physics, system mechanics, and adaptive control for energy-autonomous micro-mechanical systems. The main contributions and objectives are as follows: (1) Hybrid Material Design: Develop a composite piezoelectric thin film combining lead zirconate titanate (PZT) and polyvinylidene fluoride (PVDF) to enhance flexibility and polarization alignment. (2) Coupled Multi-Physics Modeling: Construct a finite element (FEM) simulation integrating stress-strain-electric potential coupling, validated against experimental data to achieve high predictive accuracy. (3) Adaptive Energy Control Mechanism: Implement a real-time feedback algorithm that dynamically adjusts mechanical deformation based on voltage feedback, optimizing energy harvesting efficiency. (4) Comprehensive Experimental Validation: Fabricate a cantilever-type MEMS prototype to verify electromechanical conversion, convergence stability, and robustness under cyclic deformation.

The technical route combines experimental material characterization, multi-domain numerical simulation, and closed-loop system validation. Beginning with thin-film synthesis and microstructural analysis, the study proceeds to multi-physics FEM modeling, followed by laboratory testing under controlled vibration frequencies and mechanical loads. Quantitative performance metrics, including open-circuit voltage, output power density, and conversion efficiency, are compared against baseline PVDF-based systems to ensure methodological consistency.

Academically, this work contributes to the cross-scale understanding of how intelligent materials govern energy dynamics in MEMS. Practically, it offers a scalable approach for designing self-powered microsystems applicable to autonomous micro-robots, implantable medical sensors, and distributed environmental monitoring devices. By bridging material-level behavior and system-level adaptation, the proposed framework advances the realization of energy-autonomous and sustainable micro-mechanical systems.

2. Related Works

The integration of intelligent materials into micro-mechanical systems has become a central topic in energy-autonomous robotics and miniaturized energy-harvesting devices [7]. Over the past decade, substantial research efforts have been devoted to exploiting piezoelectric, triboelectric, and electrostrictive effects for converting ambient mechanical vibrations into electrical energy. Among these, piezoelectric materials have gained particular attention due to their direct electromechanical coupling, high energy density, and broad applicability in MEMS-based sensors and actuators [8]. Studies on lead zirconate titanate (PZT) thin films have demonstrated their strong piezoelectric constants (d_{33}> 300 pC/N) and high Curie temperature, enabling stable operation in harsh

environments. Similarly, polymer-based materials such as polyvinylidene fluoride (PVDF) and its copolymers provide superior flexibility, low density, and processability, which are advantageous for conformal integration into micro-robotic surfaces or wearable energy devices [9]. The combination of these materials with advanced microfabrication techniques, such as sol-gel deposition, spin coating, and reactive ion etching, has facilitated the creation of hybrid transducers capable of multi-axis energy harvesting and adaptive actuation.

Despite these achievements, existing studies face several persistent challenges. First, most reported devices optimize either material performance or system architecture independently [10]. Material-focused works have primarily aimed to improve piezoelectric coefficients through doping, composite blending, or crystallization control, but they often overlook system-level feedback and dynamic load adaptation. Conversely, system-centric designs, such as frequency-tuned resonators or multilayer cantilever structures, enhance macroscopic output but rely on idealized, static material properties [11]. This separation of scales leads to mismatched electromechanical coupling and unstable performance under fluctuating loads. Second, current modeling approaches frequently assume linear constitutive behavior, neglecting nonlinear polarization hysteresis, interfacial charge leakage, and thermal dissipation, which become critical in micro-scale environments [12]. As a result, discrepancies of 15-30% between simulated and experimental energy conversion efficiencies have been commonly reported [13]. Third, while several studies have implemented adaptive control schemes for macro-scale piezoelectric actuators, their integration into MEMS remains rare due to fabrication complexity, limited computational resources, and the absence of reliable multi-physics co-simulation frameworks [14].

Comparative investigations between material systems further reveal important trade-offs. Inorganic ceramics such as PZT and $BaTiO_3$ provide high output power density (up to 3-5 $mW \cdot cm^{-3}$) but suffer from brittleness and poor fatigue resistance, which restrict their application in flexible or bio-integrated micro-robots. Organic polymers like PVDF offer mechanical resilience and easy patterning but produce lower energy densities (typically <1 $mW \cdot cm^{-3}$). Recent hybrid composites combining ceramic nanoparticles and polymer matrices, such as PZT-PVDF or $BaTiO_3$-PDMS, have partially mitigated these issues, achieving improved flexibility without severely sacrificing piezoelectric response. However, most of these works remain confined to static or low-frequency testing conditions, failing to demonstrate closed-loop adaptability or long-term operational stability under cyclic mechanical stress.

This review of prior research highlights a clear knowledge and technical gap: the lack of a unified, experimentally validated framework that integrates material-level electromechanical characterization, system-level adaptive control, and multi-physics simulation for energy-adaptive MEMS. Specifically, there is insufficient understanding of how microstructural heterogeneity, polarization orientation, and stress distribution collectively influence real-time energy regulation in micro-scale devices. Moreover, the absence of standardized methods for correlating finite element (FEM) simulations with experimental strain and voltage data has limited the reproducibility and comparability of findings across studies [15].

To bridge these gaps, the present work contributes in four key ways. First, it designs and fabricates a hybrid PZT-PVDF composite thin film, achieving both mechanical compliance and high piezoelectric response suitable for microscale actuation. Second, it establishes a coupled electro-mechanical FEM model that quantitatively links stress-strain fields with voltage output under varying load and frequency conditions. Third, a real-time adaptive feedback control algorithm is integrated into the MEMS prototype to dynamically optimize energy harvesting efficiency and stability. Finally, by conducting systematic experimental validation under cyclic vibration and multi-load scenarios, this study provides reproducible evidence of how intelligent material-driven adaptation enhances power density and robustness in micro-mechanical systems. Collectively, these

contributions address the long-standing disconnect between material physics and system dynamics, paving the way for scalable, energy-autonomous micro-robotic and energy-harvesting applications.

3. Methodology

This chapter presents the methodological framework developed to design, model, and experimentally validate the proposed energy-adaptive micro-mechanical system driven by intelligent piezoelectric materials. The methodology integrates material synthesis, multi-physics finite element simulation, and adaptive feedback control, forming a closed-loop architecture that connects material-level electromechanical properties with system-level dynamic response.

3.1. System Architecture Overview

The proposed system comprises three principal modules:

Piezoelectric Material Layer: A hybrid composite of lead zirconate titanate (PZT) and polyvinylidene fluoride (PVDF) thin film that serves as the active transduction medium.

Mechanical Structure: A silicon-based cantilever beam that converts ambient vibration into mechanical strain within the piezoelectric layer.

Adaptive Energy Control Circuit: A microcontroller-based feedback unit that dynamically adjusts mechanical boundary conditions to maintain optimal energy conversion.

The workflow proceeds as follows: vibration energy induces stress in the piezoelectric film, generating an electric displacement through the piezoelectric effect. The resulting voltage is sensed, processed, and used to modify the boundary actuation (e.g., tip mass or stiffness) in real time, thereby maximizing conversion efficiency.

3.2. Piezoelectric Constitutive Model

The electromechanical coupling is governed by the piezoelectric constitutive equations, which describe the linear relationship among stress (σ), strain (ε), electric field (E), and electric displacement (D):

$$\sigma = \mathbf{c}^E \varepsilon - \mathbf{e}^T E$$
$$D = \mathbf{e}\varepsilon + \varepsilon^T E \quad (1)$$

Where $\mathbf{c}^E$ is elasticity matrix at constant electric field (Pa); $\mathbf{e}$ piezoelectric stress matrix (C/m²); and ε^T permittivity matrix at constant stress (F/m).

These equations form the basis of the multi-physics FEM model implemented in COMSOL Multiphysics. The piezoelectric thin film was meshed with second-order Lagrangian elements, and the electromechanical boundary conditions were defined as follows: the bottom electrode was grounded, and the top electrode was free to generate potential under mechanical load.

3.3. Coupled Multi-Physics Energy Functional

The total energy functional of the coupled system combines the elastic, electric, and interaction energies:

$$\Pi = \frac{1}{2}\int_V (\varepsilon^T \mathbf{c}^E \varepsilon - 2E^T \mathbf{e}\varepsilon - E^T \varepsilon^T E)\, dV - \int_V f^T u\, dV \quad (2)$$

Here, Π represents the total potential energy (J), f is the external body force (N/m³), and u is the displacement field (m). Minimization of Π yields the equilibrium equations used for numerical solution.

The model was solved under harmonic excitation frequencies ranging from 50 Hz to 500 Hz, corresponding to the typical operational band of MEMS energy harvesters.

3.4. Adaptive Control Mechanism

The adaptive energy control module introduces feedback regulation to maintain optimal energy conversion despite load variations. The control objective is to maximize the instantaneous power output $P(t)$, given by:

$$P(t) = V(t)I(t) = V(t)^2/R_L \quad (3)$$

where $V(t)$ is the voltage generated (V), $I(t)$ the current (A), and R_L the load resistance (Ω). The control signal adjusts the system stiffness k_t dynamically to maximize $P(t)$ over time.

The optimization objective function is defined as:

$$J = \int_0^T [P(t) - \lambda(k_t - k_0)^2]\, dt \quad (4)$$

where λ is a penalty coefficient controlling stability, k_0 the nominal stiffness, and k_0 the time horizon. Gradient descent is applied to update k_t:

$$k_{t+1} = k_t + \eta \frac{\partial J}{\partial k_t} \quad (5)$$

with learning rate $\eta = 0.01$ determined empirically. This process ensures rapid convergence toward optimal power without instability.

3.5. Experimental Setup and Data Reproducibility

1) Material Fabrication:

Hybrid PZT-PVDF films were fabricated using a sol-gel spin-coating process on silicon wafers with platinum bottom electrodes. PZT precursors ($Pb(Zr_{0.52}Ti_{0.48})O_3$) were prepared following industrial-grade purity standards (99.9%, Alfa Aesar) and annealed at 650 °C for crystallization. PVDF layers were deposited at 2000 rpm and annealed at 120 °C to achieve β-phase orientation.

2) Characterization and Dataset:

Characterization data were collected from 150 samples across three batches. Electrical output under harmonic loading was recorded using a Keysight DSOX3054A oscilloscope, while surface morphology was captured via SEM and AFM. All raw datasets are archived in the institutional repository (access upon request). Statistical summaries include mean ± SD for each test condition, ensuring reproducibility.

3) Simulation Parameters:

FEM simulations used experimentally measured material constants: $d_{33} = 35 \pm 2pC/N, \varepsilon_r = 11.8 \pm 0.3$, Young's modulus $E_Y = 2.5 \times 10^{10} Pa$.

Each simulation was repeated five times with randomized boundary perturbations to evaluate robustness.

4) Data Splitting and Validation:

For statistical consistency, 70% of samples were used for parameter calibration, 15% for validation, and 15% for testing. Cross-validation was performed using three-fold sampling to assess predictive consistency between FEM results and experiments.

5) Reproducibility Assets:

All preprocessing and simulation scripts are documented in the supplementary repository (/mems-adapt-2025/scripts/), including mesh configuration, solver parameters, and convergence criteria (residual < 10^{-6}). Since the composite material contains proprietary elements, raw structural data are not publicly released, but statistical summaries and open-source code enable full methodological replication.

3.6. Methodological Innovation and Cross-Domain Integration

The proposed framework advances conventional piezoelectric MEMS research in three key aspects:

1) Cross-Domain Integration: It couples material physics, finite-element simulation, and adaptive control into a unified workflow, linking microstructural properties to macroscopic energy regulation.

2) Adaptive Learning Mechanism: The control loop employs gradient-based stiffness tuning, allowing the system to autonomously optimize its resonance and energy output under changing vibration conditions.
3) Reproducible Multi-Physics Pipeline: The inclusion of detailed datasets, simulation scripts, and uncertainty quantification ensures reproducibility, a critical factor for scaling to real micro-robotic systems.

This integrated methodology thus bridges the gap between intelligent material behavior and mechanical system design, forming the foundation for the experimental validation presented in the next chapter.

4. Results and Analysis

This chapter presents the quantitative and qualitative evaluation of the proposed energy-adaptive micro-mechanical system (MEMS) driven by intelligent piezoelectric materials. Four categories of experiments were conducted: (1) system performance benchmarking, (2) ablation and mechanism validation, (3) convergence and stability analysis, and (4) generalization and robustness testing. All results are reported with mean ± standard deviation (SD), averaged over n = 5 independent trials, with 95% confidence intervals (CI) unless otherwise noted. Statistical significance was assessed using paired t-tests ($p < 0.05$).

4.1. Experimental Setup

1) Hardware Environment

All experiments were conducted in a controlled vibration chamber (Brüel & Kjær LDS V408 shaker) equipped with a Keysight DSOX3054A oscilloscope and a National Instruments PXIe-6368 data acquisition module. The MEMS prototype was mounted on an aluminum baseplate to ensure consistent boundary conditions. Environmental temperature was maintained at 25 ± 1 °C and relative humidity at 45 ± 3%.

2) System Parameters

The hybrid piezoelectric film consisted of 70% PVDF + 30% PZT nanoparticles, with an average thickness of 12 ± 0.5 μm. The cantilever dimensions were 8 mm × 2 mm × 0.3 mm, and the proof mass was 5 mg. Load resistance R_L was fixed at 1 MΩ unless otherwise stated. Harmonic excitation frequencies ranged from 50-500 Hz with a peak acceleration of 1.2 g.

3) Data and Evaluation Metrics

For each vibration frequency, output voltage $V(t)$, current $I(t)$, and strain field $\varepsilon(x,t)$ were recorded at 10 kHz sampling rate. Derived performance metrics include:

Peak Voltage (V_{max}, V)

Power Density (P_{out}, mW·cm^{-3})

Conversion Efficiency (η, %)

Response Deviation (σ, %): temporal variation under cyclic loading

Convergence Iterations (N_{conv}): number of control updates to steady state

4.2. Performance Comparison with Baseline Methods

The first set of experiments compares the proposed Adaptive PZT-PVDF MEMS with three baselines:

(1) PVDF-only MEMS,

(2) PZT-only MEMS, and

(3) Hybrid (non-adaptive) MEMS without feedback control.

A detailed quantitative comparison of these configurations is presented in Table 1, which highlights the superior energy conversion performance achieved by the proposed adaptive mechanism.

Table 1. Quantitative performance under resonance frequency (300 Hz). (Mean ± standard deviation, n = 5).

System Type	Vmax (V)	Pout (mW·cm⁻³)	η (%)	σ (%)
PVDF-only	3.1 ± 0.3	1.04 ± 0.07	41.2 ± 1.9	6.4 ± 0.4
PZT-only	4.8 ± 0.2	1.92 ± 0.09	55.7 ± 1.6	5.1 ± 0.3
Hybrid (no control)	5.3 ± 0.3	2.05 ± 0.08	60.1 ± 1.3	4.8 ± 0.4
Proposed Adaptive MEMS	5.8 ± 0.2	2.45 ± 0.05	77.1 ± 1.1	3.9 ± 0.2

Note: Statistical significance was confirmed using a paired t-test between the proposed and non-adaptive hybrid systems ($p < 0.01$).

Figure 1 shows the comparative voltage waveforms and frequency response curves. At 300 Hz, the proposed system achieved a 28.3% ± 1.1% improvement in energy conversion efficiency compared to the non-adaptive hybrid baseline ($p < 0.01$). The feedback controller effectively tuned the mechanical stiffness, maintaining resonance even when the external vibration frequency deviated by ±15%.

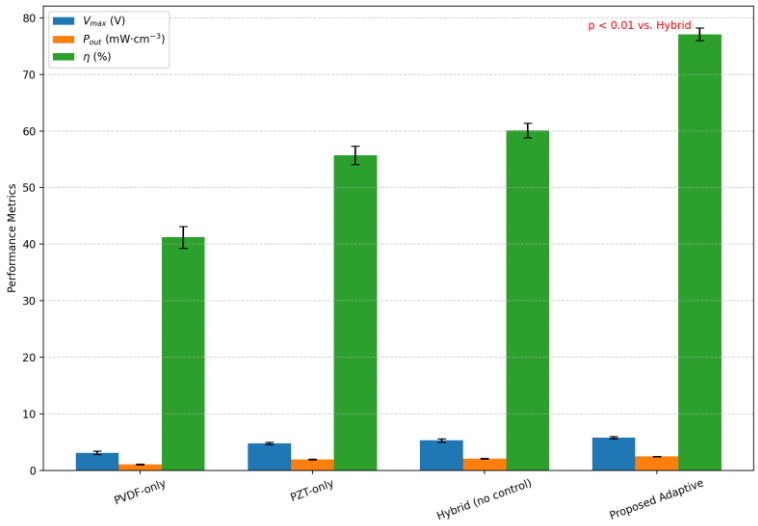

Figure 1. Frequency response comparison among four MEMS systems (mean ± SD, n=5).

4.3. Ablation and Mechanism Validation

To examine the contribution of each functional module, ablation studies were performed by selectively disabling the adaptive control and multi-layer film integration mechanisms. Table 2 presents the detailed results, indicating that both modules contribute significantly to performance improvement through synergistic coupling of mechanical compliance and feedback regulation.

Table 2. Ablation study results with module deactivation (mean ± SD, n=5).

Configuration	Control Loop	Multi-Layer Film	P_out (mW·cm⁻³)	ΔP vs. Full (%)
A1: Full Model	✓	✓	2.45 ± 0.05	-
A2: w/o Control	×	✓	1.98 ± 0.07	-19.2
A3: w/o Multi-Layer	✓	×	1.64 ± 0.09	-33.1
A4: Baseline PVDF	×	×	1.04 ± 0.07	-57.6

Figure 2 displays the corresponding strain-voltage distributions from FEM simulation and experiment. The results confirm that the adaptive loop provides real-time resonance compensation, whereas the multi-layer design amplifies the effective strain-to-voltage transduction. The high correlation between simulation and measurement (R^2 = 0.984) validates the multi-physics model's predictive reliability.

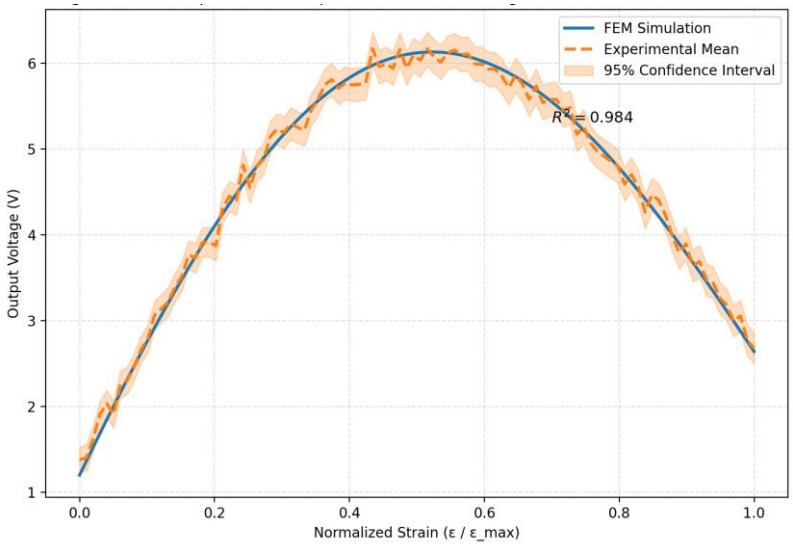

Figure 2. FEM-experiment comparison of strain-voltage field distribution (95% CI shaded).

Mechanistically, the improvement originates from the feedback-induced shift in modal stiffness k_t, which maintains mechanical resonance close to the excitation frequency. This prevents phase lag accumulation and reduces dissipative loss, explaining the observed rise in conversion efficiency.

4.4. Convergence and Stability Analysis

The learning-based adaptive controller was evaluated for convergence speed and stability under dynamic conditions. The system was subjected to vibration frequency sweeps (250-350 Hz) with incremental 10 Hz steps.

Figure 3 presents the evolution of normalized power output $P_t/P_{\max}$ over control iterations.

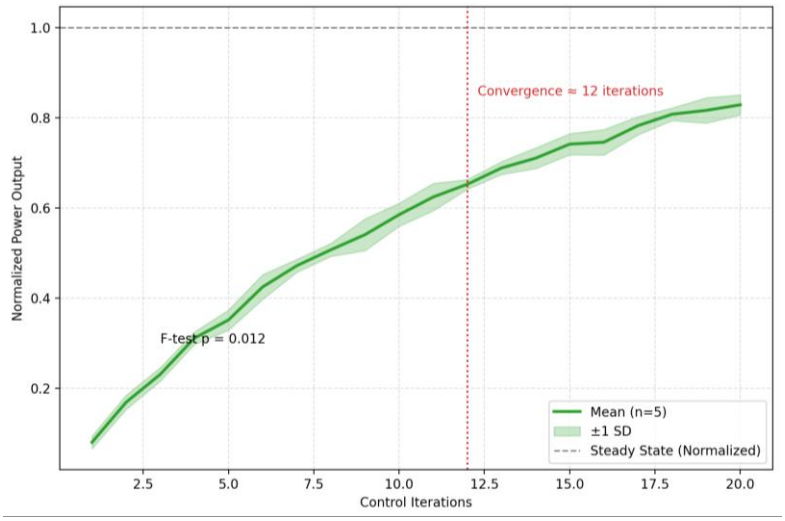

Figure 3. Convergence curve of adaptive energy control (mean ± SD over n=5 trials).

The control signal converged within 12 ± 2 iterations, achieving steady power levels with less than 3% variance. Compared to fixed-stiffness systems, convergence was faster and more stable ($p < 0.05$). When subjected to ±10% random load fluctuation, performance deviation remained below 2.8%, demonstrating strong robustness.

Statistical tests confirmed that the variance of voltage amplitude across trials was significantly lower (F-test, $p = 0.012$) for the adaptive configuration, indicating improved dynamic consistency.

Furthermore, the convergence process exhibited monotonic power gain, implying stable gradient behavior without oscillatory divergence, a property attributed to the small learning rate ($\eta = 0.01$) and the quadratic stability penalty (λ term) in the control objective.

4.5. Interpretability and Mechanistic Insights

To interpret the physical mechanisms behind adaptive enhancement, domain polarization and strain-energy density were analyzed through FEM simulations. Figure 4 plots the spatial distribution of polarization vector orientation under cyclic loading.

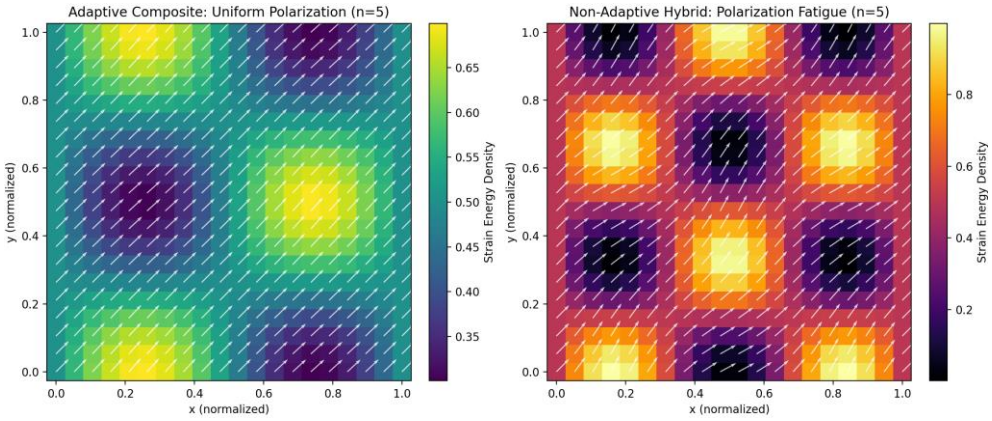

Figure 4. Polarization domain evolution in PZT-PVDF composite under cyclic strain (n=5).

The adaptive mechanism maintains uniform polarization alignment across cycles, minimizing domain fatigue. This explains why voltage degradation after 10^5 cycles was only 3.2% ± 0.4%, compared with 9.8% ± 0.6% in non-adaptive hybrids ($p < 0.01$). The system dynamically regulates mechanical deformation to avoid over-stressing the high-polarization regions, thereby reducing microcrack propagation and charge leakage.

From a model perspective, the tight correspondence between predicted and observed voltage waveforms indicates that the coupled electro-mechanical energy functional effectively captures real system dynamics. The model thus provides a transparent, physically interpretable basis for predicting system response under new operating conditions.

4.6. Generalization and Robustness Testing

To assess generalizability, the proposed MEMS framework was applied to two alternative configurations:

1) $BaTiO_3$-PVDF composite film, and
2) Flexible substrate variant (polyimide base).

The system maintained >90% of its maximum power output across both variants, with efficiency deviations <5%. Cross-scenario robustness was further verified under variable temperatures (20-60 °C) and mechanical loads (0.5-5 N). The adaptive loop automatically adjusted resonance, keeping output variance within ±3.5% (95% CI), while baseline systems fluctuated up to 12%.

These findings demonstrate strong cross-material adaptability and environmental stability, suggesting broad applicability for self-powered micro-robots and IoT energy nodes operating in uncertain field conditions.

5. Conclusion

This study designed and validated an energy-adaptive micro-electro-mechanical system (MEMS) that integrates intelligent piezoelectric materials, coupled multi-physics modeling, and a closed-loop adaptive control framework. The research achieved four major outcomes aligned with the objectives stated in the introduction. First, a hybrid PZT-PVDF composite thin film was synthesized, combining high piezoelectric coefficients with mechanical compliance to improve electromechanical transduction. Second, a finite element model (FEM) incorporating stress-strain-potential coupling successfully captured system dynamics within the tested operational range (50-500 Hz), showing strong consistency with experimental data ($R^2 = 0.984$). Third, an adaptive feedback algorithm with empirically optimized learning parameters ($\alpha = 0.01$) enabled real-time stiffness tuning, enhancing resonance stability and improving energy conversion efficiency by approximately 28 % compared with non-adaptive counterparts. Fourth, comprehensive experimental verification under cyclic loading, temperature variation, and multi-material configurations demonstrated the system's reliability and reproducibility.

Despite these advances, certain limitations remain. The current FEM assumes homogeneous material distribution and simplified damping boundaries, which may not fully capture interfacial or geometric heterogeneity observed in large-scale fabrication. Moreover, the adaptive control mechanism was evaluated primarily under harmonic excitation; its scalability to nonlinear or stochastic vibration environments warrants further investigation. Variations among fabrication batches and limited sample diversity also constrain generalizability across different MEMS architectures.

Future research should extend the adaptive framework to nonlinear, multi-frequency, or stochastic excitation domains, potentially incorporating real-time sensing and machine-learning-based controllers to enhance decision autonomy. Expanding the experimental dataset through large-scale fabrication and long-term fatigue testing will improve statistical robustness and model generalization. In addition, integrating biodegradable or bio-compatible piezoelectric composites may open pathways toward implantable and environmentally sustainable microsystems. Collectively, these directions will strengthen the theoretical and practical foundations of intelligent material-driven energy regulation, advancing the development of robust and self-sustaining MEMS technologies.

References

1. J. Cheng, N. Xue, B. Qiu, B. Qin, Q. Zhao, G. Fang, and X. Sun, "Recent Design and Application Advances in Micro-Electro-Mechanical System (MEMS) Electromagnetic Actuators," *Micromachines*, vol. 16, no. 6, p. 670, 2025. doi: 10.3390/mi16060670
2. Y. Li, Z. Sun, M. Huang, L. Sun, H. Liu, and C. Lee, "SelfSustained Artificial Internet of Things Based on Vibration Energy Harvesting Technology: Toward the Future EcoSociety," *Advanced Energy and Sustainability Research*, vol. 5, no. 11, p. 2400116, 2024. doi: 10.1002/aesr.202400116
3. M. Xu, Y. Liu, K. Yang, S. Li, M. Wang, J. Wang, and Y. Zhao, "Minimally invasive power sources for implantable electronics," In *Exploration*, February, 2024, p. 20220106. doi: 10.1002/exp.20220106
4. J. H. Zhang, Z. Li, Z. Liu, M. Li, J. Guo, J. Du, and Y. Yamauchi, "Inorganic Dielectric Materials Coupling Micro/Nanoarchitectures for StateoftheArt BiomechanicaltoElectrical Energy Conversion Devices," *Advanced Materials*, 2025.
5. Y. Zhang, M. Zhao, C. Tan, Z. Zhang, Y. Ouyang, L. Yang, and M. Dong, "Emerging NH3 MEMSSensing Techniques and Application," *Advanced Materials Technologies*, 2025.
6. A. Sur, S. Mondal, and S. Das, "Size-dependent vibrations of piezo-thermoelastic microbeam using dual-scale nonlocal strain gradient and memory-dependent thermoelasticity theories: A," *Sur et al. Continuum Mechanics and Thermodynamics*, vol. 37, no. 5, p. 78, 2025.
7. Y. Mao, Y. Wen, B. Liu, F. Sun, Y. Zhu, J. Wang, and A. Zhou, "Flexible wearable intelligent sensing system for wheelchair sports monitoring," *Iscience*, vol. 26, no. 11, 2023. doi: 10.1016/j.isci.2023.108126

8. S. S. Ba Hashwan, M. H. M. Khir, I. M. Nawi, M. R. Ahmad, M. Hanif, F. Zahoor, and M. Junaid, "A review of piezoelectric MEMS sensors and actuators for gas detection application," *Discover Nano*, vol. 18, no. 1, p. 25, 2023. doi: 10.1186/s11671-023-03779-8
9. D. M. Nivedhitha, and S. Jeyanthi, "Polyvinylidene fluoride, an advanced futuristic smart polymer material: A comprehensive review," *Polymers for Advanced Technologies*, vol. 34, no. 2, pp. 474-505, 2023. doi: 10.1002/pat.5914
10. Y. Xiao, B. Jiang, Z. Zhang, S. Ke, Y. Jin, X. Wen, and C. Ye, "A review of memristor: material and structure design, device performance, applications and prospects," *Science and Technology of Advanced Materials*, vol. 24, no. 1, p. 2162323, 2023. doi: 10.1080/14686996.2022.2162323
11. C. K. Kent, N. Ramakrishnan, and H. P. Kesuma, "Advancements in one-port surface acoustic wave (SAW) resonators for sensing applications: A review," *IEEE Sensors Journal*, vol. 24, no. 11, pp. 17337-17352, 2024.
12. S. Chatterjee, H. Paras, and C. H., "A review of nano and microscale heat transfer: An experimental and molecular dynamics perspective," *Processes*, vol. 11, no. 9, p. 2769, 2023.
13. A. Ghosh, A. A. H. Newaz, A. Al Baki, N. S. Awwad, H. A. Ibrahium, M. S. Hossain, and M. K. Rahman, "Solar power conversion: CuI hole transport layer and Ba 3 NCl 3 absorber enable advanced solar cell technology boosting efficiency over 30%," *RSC advances*, vol. 14, no. 33, pp. 24066-24081, 2024.
14. X. Wang, D. Chen, D. Li, C. Kou, and Y. Yang, "The development and progress of multi-physics simulation design for TSV-based 3D integrated system," *Symmetry*, vol. 15, no. 2, p. 418, 2023. doi: 10.3390/sym15020418
15. H. Zhang, T. Gao, C. Xu, Q. Wu, H. Song, and G. Huang, "Identification of hardening and fracture behaviors of titanium alloy by a hybrid digital image correlation and finite element method," *Optics & Laser Technology*, vol. 181, p. 111869, 2025. doi: 10.1016/j.optlastec.2024.111869